CLINICAL SCIENCE

Quantification of histological changes after calibrated crush of the intraorbital optic nerve in rats

Nils-Claudius Gellrich, Ronald Schimming, Martin Zerfowski, Ulf Theodor Eysel

Br J Ophthalmol 2002;**86**:233–237

See end of article for authors' affiliations

Correspondence to: Dr N-C Gellrich, Department of Oral and Maxillofacial Surgery, University Hospital of Freiburg, Hugstetterstrasse 55, D-79106 Freiburg, Germany; gellrich@zmk2.ukl.uni-freiburg.de

Accepted for publication 25 July 2001

Background: Traumatic optic nerve lesions (TONL) are probable but unpredictable consequence after severe midface or skull base trauma. Based on a previously described rat model, the authors developed a new model in order to simulate optic nerve crush during trauma on the optic canal.
Methods: To achieve a calibrated TONL, a microinjuring device was designed that made it possible to assess the correlation between a defined trauma and the neuronal degeneration in the rat retinal ganglion cell (RGC) layer. This device is based on a small dynamometer mounted onto a conventional micromanipulator. The supraorbital approach was chosen to expose the extracranial optic nerve.
Results: In this rat model (n=100, Wistar strain) the parameters of "force" and "time" could be precisely monitored during the experiment. The decrease in the mean number of retinal neurons (N) according to the pressure exerted (2–30 $cN \cdot mm^{-2}$) on the optic nerve was linear for 1, 6, and 15 minutes of injuring time; the decrease in N for varying injuring forces also appears to be nearly linear.
Conclusion: The results show that this model provides a reliable method for studying quantitatively the anatomical effects of TONL on the RGC layer and the optic nerve itself, and may allow the design of treatment strategies following TONL.

Several groups have studied the histological, electrophysiological, pathophysiological and behavioural effects of optic nerve trauma. Our goal was to create a method that simulated trauma to the optic nerve caused by fractures of the midface and/or skull base, in order to investigate from a histological point of view the effects of calibrated optic nerve crush.

The main drawback of most of the methods described for calibrated optic nerve trauma is that the injuring trauma cannot be directly quantified at the site of the lesion, but is rather semiquantitatively referred to as pressure in a balloon,[1–3] distance between branches of a forceps,[4 5] or pulling force on a micro sling.[6]

Several other reports on traumatic optic nerve lesions (TONL) based on crushing of the optic nerve have been published in which the force applied was not stated.[7–10]

The balloon method was used on the optic nerve of the cat[1–3] and the micro sling was used on the optic nerve of Japanese monkeys.[6] Forceps were used to cause a defined trauma to the optic nerve of rats.[4 5] For insertion of the crushing forceps, the optic nerve was approached via a lateral canthotomy and an incision of the conjunctiva lateral to the cornea.[5] Taking into account that the optic nerve of the rat is a very vulnerable structure approximately 0.64 mm in diameter, a standardised crush model is mandatory to guarantee defined and reliable conditions for later microscopic or electrophysiological evaluation of the post-traumatic changes in the retinal ganglion cell (RGC) layer.

Table 1 Indirect light reaction of the uninjured eye immediately postoperative (ILR) and 30 days later (ILR30) in relation to force exerted and duration of TONL. Results are arithmetical means; individually, each positive ILR was counted as 1, each negative ILR was taken as 0

TONL	n	ILR	ILR30
0 cN	10	0.7	1
2 cN 6 minutes	3	0.3	1
2 cN 15 minutes	3	0	1
2 cN 30 minutes	3	0.7	1
5 cN 1 minute	8	0.9	1
5 cN 6 minutes	7	0.7	1
5 cN 15 minutes	6	0.3	1
5 cN 30 minutes	4	0.3	1
10 cN 1 minute	9	0.3	1
10 cN 6 minutes	5	0.2	1
10 cN 15 minutes	4	0	0.5
10 cN 30 minutes	5	0	0.4
15 cN 1 minute	11	0.2	0.9
15 cN 6 minutes	6	0.2	0.3
15 cN 15 minutes	4	0	0
20 cN 6 minutes	6	0	0.2
30 cN 1 second	6	0	0.2

MATERIALS AND METHODS

Surgical procedure

Male albino rats of the Wistar strain (n = 100) weighing 300–350 g were anaesthetised using 40 mg chloral hydrate in water per 100 g body weight. The head was fixed in a stereotaxic frame. The supraorbital rim was exposed through a median frontal skin incision. Preserving the supraorbital vein, the retrobulbar space was entered and almost all the Harderian gland removed. Thus, the muscle cone comprising the ocular muscles was easily accessible. While carefully dislocating the eyeball anteriorly, the ocular muscles overlying the optic nerve could be separated and held apart with a forked micro hook, so that only the retractor bulbi muscle remained around the optic nerve. Care was taken to preserve retinal perfusion during this manoeuvre of anterior dislocation. Next, the retractor bulbi was cut 2 mm behind the posterior surface of the eyeball and removed from the optic nerve. Without damaging the optic nerve, a micro hook was inserted from above, with its surface parallel to the nasal aspect of the optic nerve. Throughout these operative steps, retinal perfusion was monitored by funduscopy of the operated eye. Indirect light (ILR)

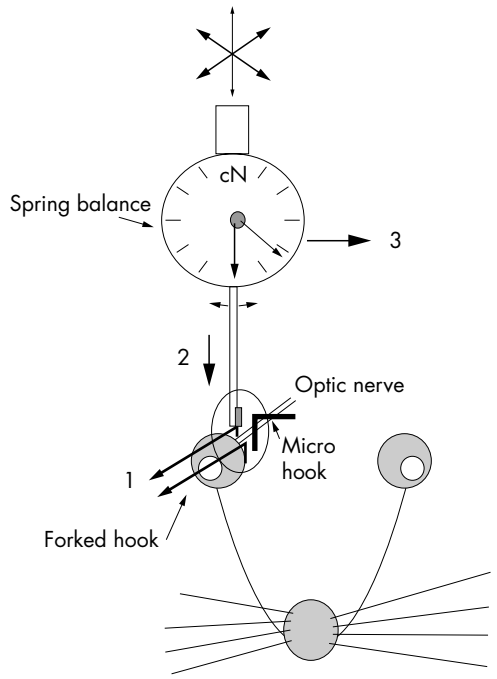

Figure 1 Experimental set up with microinjuring device (dynamometer: 0–6 cN, 3–30 cN; dial plate diameter, 37 mm; separate pointer indicating maximum force).**1**, anterior luxation of the eyeball; **2**, insertion of the dynamometer arm; **3**, injuring of the optic nerve by moving the dynamometer with the micromanipulator

was assessed in the unoperated eye before surgery, in the immediate postoperative period, and after 30 days (ILR30) (Table 1).

Microinjuring device

Using a metallic micro hook adapted with adhesive wax to a three dimensionally adjustable supranasal metal pin, it was possible to create one branch of the assumed forceps (Fig 1). The insertion and positioning of the micro hook parallel to the optic nerve of the rat could easily be done through the supraorbital approach.

A small dynamometer (dial plate diameter, 37 mm; range of force, 3–30 cN or 1–6 cN; separate pointer indicating maximum force; Correx, Haag-Streit AG, Bern, Switzerland, No 44106) was attached to a conventional micro-manipulator. A polished microplate (1×2 mm^2) was mounted on the tip of the dynamometer. Thus, the microinjuring device could be moved with the micro-manipulator close to the temporal aspect of the optic nerve and opposite the metal hook placed on the nasal aspect of the optic nerve, so that the principle of a forceps was completed.

Calibrated optic nerve trauma

Using the above described microinjuring device, a calibrated trauma was inflicted on the right optic nerve of all the rats (n = 100). The left retinas were used as controls (K; n = 23). The effect of the optic nerve preparation and the installation of the microinjuring device were evaluated on a group of 10 sham operated animals (P). Table 2 shows the distribution of the applied force and the associated time of injuring. In all cases, post-injury survival time was 30 days.[11]

Histological evaluation

Thirty days after inflicting the injury, deep anaesthesia was induced with an overdose of 4% chloral hydrate. While still alive, the animals were perfused with 0.2% liquimine in Ringer-lactate solution, followed by a fixative containing 4% paraformaldehyde, and were then killed. The eyes and the intraorbital optic nerves of operated and control sites were removed and fixed for 24 hours. Then, the retinas were

Table 2 Neuron count in the RGC layer. Distribution of neurons in the RGC layer for each area evaluated—ie, central, intermediate and peripheral in percentage of the total number of neurons and mean neuron size in relation to TONL

	Number of neurons (SEM)	Neurons per counting area in % of N_{ges}; ([% of neurons ⩾ 80 µm^2])			Mean neuron size (µm^2) (SEM)			
TONL (number of animals)	Mean total number	Central	Intermediate	Peripheral	Mean size	Central	Intermediate	Peripheral
K (n=23)	230 236 (3711)	40.8 [54.4]	33.5 [54.0]	25.7 [56.9]	99.41 (0.40)	95.61 (0.56)	98.19 (0.68)	107.03 (0.91)
P (n=10)	220 866 (5877)	41.6 [53.1]	34.1 [55.0]	24.7 [55.3]	98.27 (0.59)	93.80 (0.81)	97.66 (0.98)	106.56 (1.41)
2 cN/6 min (n=3)	229 123 (14 519)	37.6 [51.6]	33.9 [63.6]	28.6 [51.3]	99.54 (1.08)	99.25 (1.76)	96.11 (2.01)	102.41 (1.82)
2 cN/15 min (n=3)	217 499 (4434)	39.9 [56.7]	33.3 [57.5]	26.9 [59.0]	102.44 (1.1)	98.92 (1.55)	100.91 (1.81)	109.56 (2.55)
2 cN/30 min (n=3)	223 770 (7890)	41.6 [63.4]	33.7 [59.3]	24.6 [55.9]	105.91 (1.13)	103.63 (1.54)	106.26 (1.99)	109.27 (2.61)
5 cN/1 min (n=8)	222 946 (8259)	41.8 [58.6]	33.4 [60.8]	24.8 [65.5]	103.89 (0.66)	97.19 (0.89)	103.30 (1.14)	115.96 (1.55)
5 cN/6 min (n=7)	213 350 (10 037)	39.1 [56.1]	35.2 [58.1]	25.7 [58.8]	104.52 (0.85)	100.29 (1.25)	103.98 (1.43)	111.66 (1.86)
5 cN/15 min (n=6)	198 095 (9809)	39.8 [56.1]	34.1 [56.7]	26.1 [60.6]	105.78 (0.91)	100.54 (1.28)	105.17 (1.55)	114.56 (2.06)
5 cN/30 min (n=4)	156 425 (8517)	41.8 [49.3]	33.8 [50.2]	24.5 [50.8]	97.79 (1.16)	93.67 (1.60)	97.30 (1.91)	105.47 (2.81)
10 cN/1 min (n=9)	215 213 (8955)	40.9 [57.7]	33.1 [58.6]	25.9 [60.0]	103.69 (0.66)	98.90 (0.90)	104.27 (1.20)	110.48 (1.48)
10 cN/6 min (n=5)	195 629 (3623)	40.7 [58.3]	33.2 [59.1]	26.0 [57.7]	107.57 (0.96)	103.69 (1.39)	108.99 (1.68)	111.82 (2.07)
10 cN/15 min (n=4)	165 443 (1691)	39.8 [46.0]	31.6 [51.2]	28.6 [49.1]	96.56 (1.09)	89.99 (1.57)	101.53 (2.06)	100.20 (2.09)
10 cN/30 min (n=5)	153 562 (10 438)	39.5 [29.1]	35.2 [32.4]	25.3 [31.5]	76.71 (0.90)	73.49 (1.42)	76.99 (1.45)	81.37 (1.92)
15 cN/1 min (n=11)	186 650 (10 240)	38.9 [53.4]	33.8 [51.2]	27.2 [58.9]	101.58 (0.66)	97.30 (0.95)	99.56 (1.13)	110.18 (1.41)
15 cN/6 min (n=6)	169 086 (8336)	39.3 [36.4]	32.6 [42.8]	28.1 [51.2]	90.09 (0.88)	82.34 (1.20)	91.14 (1.60)	99.77 (1.87)
15 cN/15 min (n=4)	135 465 (9011)	38.8 [17.1]	31.1 [20.1]	30.0 [29.5]	69.02 (0.88)	65.10 (1.36)	68.64 (1.59)	74.49 (1.65)
20 cN/6 min (n=6)	139 252 (7688)	38.0 [14.4]	33.8 [15.7]	28.2 [18.2]	61.94 (0.56)	60.25 (0.94)	61.62 (0.92)	64.61 (1.06)
30 cN/1 s (n=6)	151 479 (13 079)	38.2 [38.7]	33.5 [41.3]	28.3 [43.4]	82.13 (0.74)	80.16 (1.19)	83.07 (1.33)	83.71 (1.37)

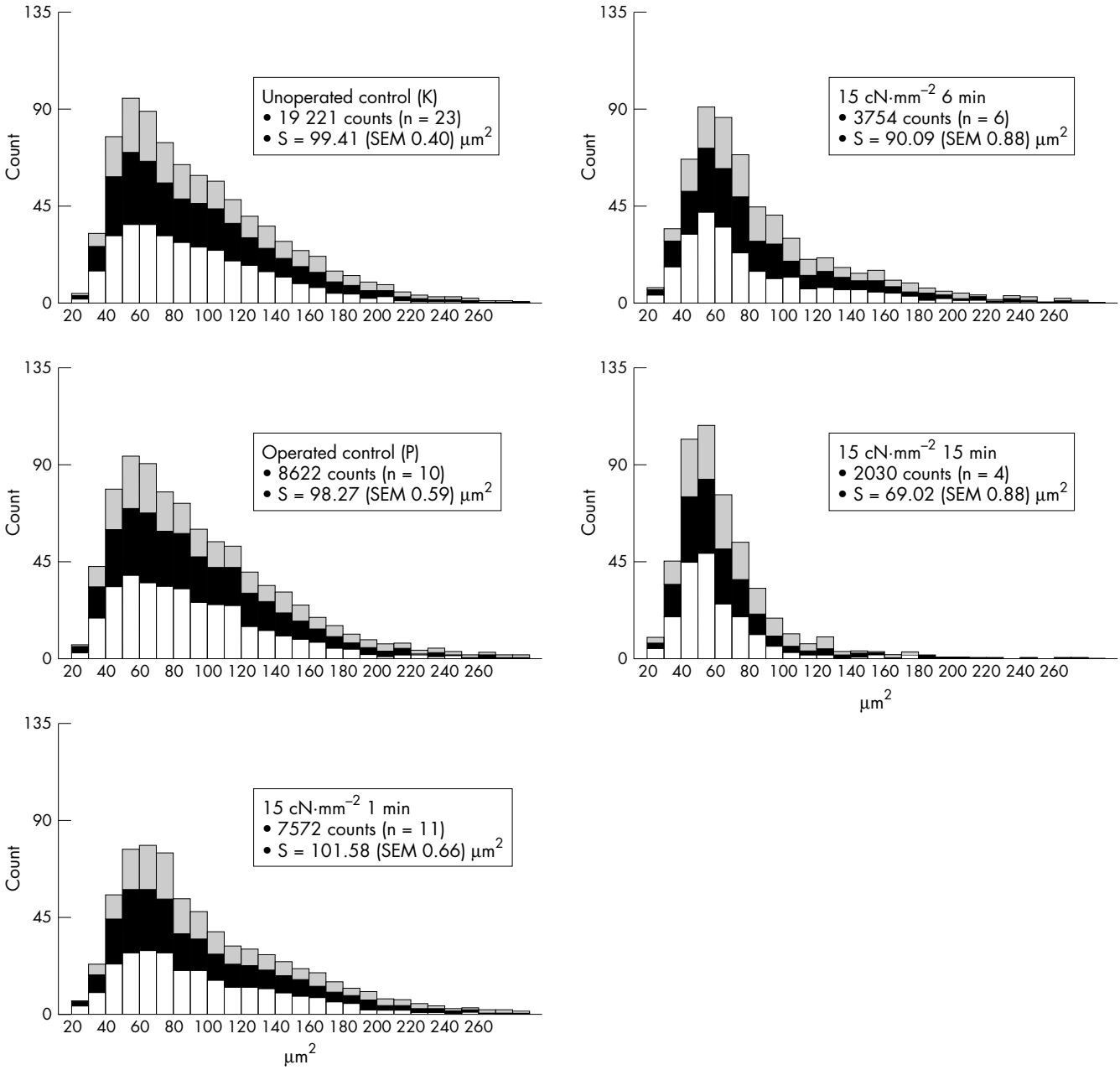

Figure 2 Histograms showing the distribution of neurons in the RGC layer in 10 µm² steps. Each column consists of three parts demonstrating the retinal central (lower row), intermediate (middle row), and peripheral (upper row) counting fields.

mounted whole onto gelatine coated slides and stained with cresyl violet. Each retina was peripherally incised to obtain five lobes. For quantitative analysis, three, 12 346 µm² counting fields (F) were defined in each lobe by drawing an axis from the papilla to the ora serrata, with three distances (1.2 mm (central), 2.4 mm (intermediate), and 3.6 mm (peripheral)) to the papilla. Neurons and glial cells were identified according to Perry's criteria.[12] In order to quantify the number and size of neurons in the RGC layer, each counting field was evaluated at 900× magnification using a camera lucida, a digitising tablet connected to a PC computer, and the Bioquant System IV software (R&M Biometrics, Inc, USA).

The total number of neurons (N) was calculated using the formula:

$N = N_C \bullet (A_R \bullet 0.8556) \bullet F^{-1}$

where

N_C = mean number of neurons per counting field

A_R = individual retina size (mm²)

$F = 0.012346$ mm² (size of each counting field)

The 0.8556 factor was calculated by Sievers *et al* and stands for the portion of the RCG layer in Wistar rats that is covered by neurons and not occupied by large intraretinal vessels.[13] A Student's *t* test was used for statistical evaluation of neurodegenerative effects.

The optic nerves were fixed for analysis during 1–2 hours in chilled, 2% osmium tetroxide fixative with 4.5% sucrose buffered with veronal acetate at pH 7.2–7.5, and embedded in Araldite. Semithin sections were stained with a solution of 1% p-phenylenediamine (PPD) in methanol-isopropanol and evaluated qualitatively by studying the degree of myelin changes.[14]

RESULTS

In all cases of TONL, reperfusion of the temporarily interrupted retinal circulation resumed at once after relieving compression of the optic nerve. During compression, the optic nerve was flattened to a structure limited by the resistance of its nerve sheath. The diameter of the injured optic nerve could be estimated as

$\frac{1}{2} \times \text{circumference}_{\text{optic nerve}} = \pi \times r_{\text{optic nerve}}$

In this series, the mean diameter of the rat optic nerve was 0.64 mm, so that during compression, the diameter of the

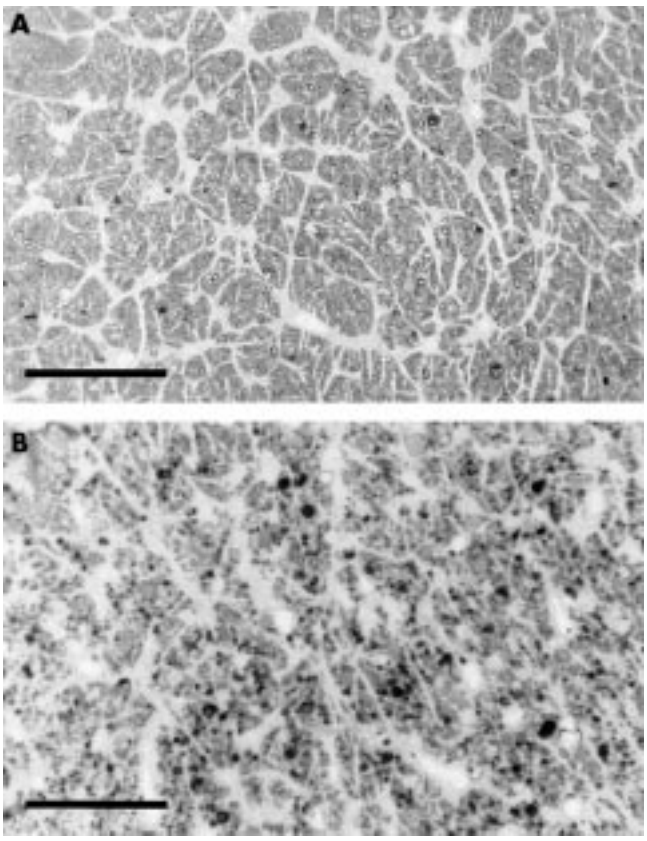

Figure 3 PPD stained semithin transverse optic nerve sections from the control group (K; (A)) and after TONL of 15 cN•mm^{-2} for 6 minutes (B). Reference scale, 100 µm.

flattened optic nerve was estimated at 1 mm. Using a 1 mm wide plate mounted on the tip of the spring balance, an injured area of 1 mm^2 follows in case of complete flattening of the optic nerve.

Figure 2 summarises the neuronal changes in the RGC layer 30 days after TONL for each group. The mean size of the retina was 59.4 (SEM 0.486) mm^2 (n = 100). The mean total number of neurons in the 23 control animals (N_K) was estimated to be 230 236 (SEM 3711). This showed no statistically significant difference at $p<0.05$ to the group of animals on which sham surgery had been performed (N_P = 220 866 (SEM 5877)) (Fig 2). Neither did the mean neuron size (S) in the RGC layer show any statistically significant difference at $p<0.05$ between the controls (S_K = 99.4 (SEM 0.4) µm^2) and those subject to sham surgery (S_P = 98.3 (SEM 0.6) µm^2).

Figure 2 additionally outlines the proportion of each evaluation area (central, intermediate, or peripheral) in relation to the total retinal number of neurons and mean neuron size. Throughout roughly all the TONL groups, the proportion of the three evaluation areas does not differ in comparison with the distribution in unoperated animals (K)— that is, the more central the retinal area is the higher the neuron density and the larger the mean neuron size. Furthermore, the proportion of neurons ≥80 µm^2 is emphasised, because those are the neurons that most probably represent RGC, whereas neurons <80 µm^2 more probably correspond to the amacrine cells.

Regarding the number of neurons (N) in the RGC layer, an injury of 15 cN•mm^{-2} for 15 minutes is followed by a neuronal degeneration similar to axotomy.[13] An injury of 2 cN•mm^{-2} was not followed by a significant reduction ($p>0.05$) in N regarding the chosen periods of injuring; neither did TONL of 5 cN•mm^{-2} over 1 and 6 minutes show any significant decrease of N. Comparison of 5, 10, 15, and 20 cN•mm^{-2} TONL reveals that neuron death directly correlates with both the force applied *and* the duration of the optic nerve lesion.

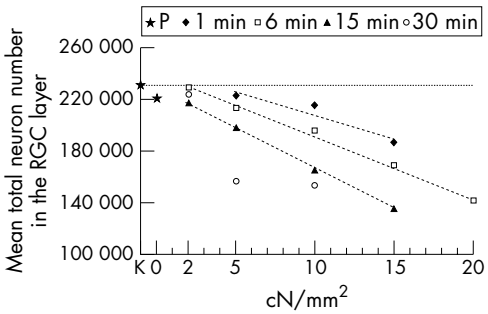

Figure 4 Mean total number of neurons in the RGC layer in relation to intensity of TONL. The horizontal dotted line demonstrates the value for the control group (K).

Pressure of 5 cN•mm^{-2} over a period of 15 minutes resulted in an RGC loss of about 32.5%, whereas pressure of 15 cN•mm^{-2} over a period of 15 minutes resulted in an RCG loss of 82.5%.

The PPD stained optic nerve sections reflect only qualitatively the neurodegenerative response to TONL. When living axons are observed, the circumference of the axon cylinder is clearly outlined by a thin dark line; in case of degeneration, the inner and outer parts of the axon cylinder cannot be differentiated and appear black (Fig 3).

Figure 4 summarises the decrease in the mean number of neurons in the retina depending on the pressure exerted on the optic nerve. Decrease in N was linear for 1, 6, and 15 minutes of injury time.

Furthermore, Table 2 shows that TONL not only affects the number of RGC, but that cell size is also modulated by the trauma. In case of TONL ≤10 cN•mm^{-2} with t ≤6 minutes or with TONL = 15 cN•mm^{-2} for 1 minute, S increases. After TONL ≥ 15 cN•mm^{-2} for ≥6 minutes, S decreases; a reduction of N ≥28% is followed by S <98 µm^2 (S_P = 98.3 µm^2). According to our data, obtained 30 days after the trauma, the distance between the site of TONL and RGC has no influence on the response of neurons in terms of neuron number and size.

Light reaction

Indirect light reaction (ILR) of the contralateral, unoperated eye was assessed at the end of the operation and compared with pupil function before perfusion with paraformaldehyde—that is, 30 days post-TONL. Absent ILR after the operation proved to be an unreliable parameter to predict the expected degree of degeneration in the RGC layer 30 days post-TONL. On the other hand, a normal ILR after TONL indicated a loss under 45.9% in RGC. Comparison of pupillary reflex and histological findings in the RGC layer 30 days post-TONL revealed that a decrease ≤53.1% in RGC did not influence ILR; a decrease >53.1% in RGC was not necessarily followed by an absent ILR. The lowest RGC count with an intact ILR was 24 713, equivalent to 21.5% of the normal RGC number. ILR recovered consistently in all experimental groups subject to lesions <10 cN•mm^{-2} for 15 minutes.

DISCUSSION

Several types of indirect (retrobulbar balloon) or direct (forceps, micro clips, micro sling, spring balance) injuring models have already been used in research programmes on TONL. Among the different approaches, the microinjuring method based on a small spring balance has proved to be a useful and easy to handle method that allows direct measurement and monitoring of the TONL.

This new method for calibrated TONL in combination with the supraorbital approach has several advantages in comparison with previously reported TONL methods and latero-orbital approaches. By recording the status of pupillary motor function immediately before and after injury and 30 days

post-TONL, a parameter for optic nerve function was found which is not influenced by any efferent changes in the injured eye when compared with the indirect light reaction (ILR) of the uninjured eye. The afferent pupillary defect was shown to correlate poorly with the degree of RGC loss. This might be due to the fact that an intact light reaction depends on a relatively low number of undamaged RGCs, which is reported to be around 13%, or it might be attributed to the different plasticity of type I, II, and III RGCs following experimental lesion, or else to the possibility that small RGCs projecting to the tectum may be spared by the experimental trauma.[15]

Another advantage of the method presented here is that, besides allowing a qualitative evaluation of calibrated TONL by studying PPD stained transverse sections of the optic nerve, changes in the number of surviving RGC after TONL can easily be assessed in a quantitative fashion. Contrary to axon counts in sections of the optic nerve, studying the RGC layer itself ensures that the site and level of histological evaluation are precisely the same.

Several publications have suggested that half of the total number of neurons in the rat RGC layer represent ganglion cells that do project an axon into the optic nerve, whereas the remaining half of the total neuron number comprises the amacrine cells that do not project an axon into the optic nerve.[13 16–22] In estimating the RGC number within the RGC layer data from the unoperated control retinas (total number of 115 107 each for RGCs and amacrine cells in the RGC layer) were compared with those of Sievers *et al*[13] (119 973 RGCs, according to axon counts in the optic nerve), and a difference of only 4.1% was found.

The results of this study make it possible to determine trends of changes in neuronal degeneration following calibrated optic nerve crush. Both time and pressure have influence on neuron survival. All the time periods chosen for this experiment ranged far below the critical time window of ischaemia reported for the retinal neuronal structures.[23 24] In another rat model in which protrusion of the eyeball and retinal ischaemia followed the filling of a retrobulbar microballoon, it could be demonstrated that stasis of retinal perfusion over 60 minutes did not result in a significant decrease in the number or size of RGCs.[25] Since retinal perfusion soon resumed after inflicting the injury, ischaemia probably did not play a significant part in our experimental paradigm. The extracranial visual pathway seemed to be relatively resistant to TONLs for short periods—that is, seconds. This finding may be consistent with clinical observations indicating that, despite major skull base trauma including fractures around the optic canals, the number of cases of traumatic optic neuropathy is relatively low. The various models of TONL previously published did not consider the relation between different injuring forces and varying injuring periods and their effect on neuronal degeneration.

Using the model described it is possible to show a distinct relation between TONL and histological degeneration assessed through changes in number and size of RGCs. These findings will be related in future experiments to electrophysiological changes. Based on this approach, we hope to establish quantitative criteria for optic nerve decompression surgery in humans, which are not yet available.[26]

Contrary to previously described methods, this experimental approach proved to be advantageous in showing the distinct relation between histological RGC degeneration, the force exerted ($cN \cdot mm^{-2}$), and its duration. Furthermore, conditions of the injury can be easily modified by varying the size of the microplate fixed to the tip of the dynamometer. Finally, this method might be applied in combination with electrophysiological recordings—that is, intraoperative recording of visual evoked potentials by pattern stimulus or flash light.[26]

IN MEMORIAM

This paper is dedicated to the memory of Professor Dr Werner Tielsch from Ruhr University Bochum (Germany).

This project was supported by a grant of the Deutsche Forschungsgemeinschaft DFG Ge 820/2-1. The authors wish to thank Ute Neubacher for technical assistance and Dr Emilia Picazo for her review of the manuscript.

Authors' affiliations

N-C Gellrich, R Schimming, Department of Oral and Maxillofacial Surgery, University Hospital of Freiburg, Freiburg, Germany
M Zerfowski, Department of Oral and Maxillofacial Surgery, University Hospital of Tübingen, Tübingen, Germany
U T Eysel, Department of Neurophysiology, Ruhr University, Bochum, Germany

REFERENCES

1 **Burke W**, Burne JA, Martin P. Selective block of Y optic nerve fibres in the cat and the occurrence of inhibition in the dorsal lateral geniculate nucleus. *J Physiol* 1985; **364**:81–92.
2 **Burke W**, Cottee LJ, Garvey J, *et al*. Selective degeneration of optic nerve fibres in the cat produced by a pressure block. *J Physiol* 1986; **376**:461–76.
3 **Cottee LJ**, Fitzgibbon T, Westland K, *et al*. Long survival of retinal ganglion cells in the cat after selective crush of the optic nerve. *Eur J Neurosci* 1991;**3**:1245–54.
4 **Duvdevani R**, Rosner M, Belkin M, *et al*. Graded crush of the rat optic nerve as a brain injury model combining electrophysiological and behavioral outcome. *Restor Neurol Neurosci* 1990; **2**:31–8.
5 **Sautter J**, Sabel A. Recovery of brightness discrimination in adult rats despite progressive loss of retrogradely labelled retinal ganglion cells after controlled optic nerve crush. *Eur J Neurosci* 1993;**5**:680–90.
6 **Matsuzaki H**, Kunita M, Kawai K. Optic nerve damage in head trauma: clinical and experimental studies. *Jpn J Ophthalmol* 1982;**26**:447–61.
7 **McKerracher L**, Hirscheimer A. Slow transport of the cytoskeleton after axonal injury. *J Neurobiol* 1992; **23**:568–78.
8 **Owusu-Yaw V**, Kyle AL, Stell WK. Effects of lesions of the optic nerve, optic tectum and nervus terminalis on rod precursor proliferation in the goldfish retina. *Brain Res* 1992;**576**:220–30.
9 **Blaugrund E**, Duvdevani R, Lavie V, *et al*. Disappearance of astrocytes and invasion of macrophages following crush injury of adult rodent optic nerves: implications for regeneration. *Exp Neurol* 1992;**118**:105–15.
10 **Misantone LJ**, Gershenbaum M, Murray M. Viability of retinal ganglion cells after optic nerve crush in adult rats. *J Neurocytol* 1984;**13**:449–65.
11 **Gellrich NC**, Gellrich MM, Bremerich A. Influence of fetal brain grafts on axotomized retinal ganglion cells. *Int J Oral Maxillofac Surg* 1994;**23**:403–5.
12 **Perry VH**. Evidence for an amacrine cell system in the ganglion cell layer of the rat retina. *Neurosci* 1981;**6**:931–44.
13 **Sievers J**, Hausmann B, Berry M. Fetal brain grafts rescue adult retinal ganglion cells from axotomy-induced cell death. *J Comp Neurol* 1989;**281**:467–78.
14 **Holländer H**, Vaaland JL. A reliable staining method for semi-thin sections in experimental neuroanatomy. *Brain Res* 1968;**10**:120–6.
15 **Bähr M**, Wizenmann A, Thanos S. Effect of bilateral tectum lesions on retinal ganglion cell morphology in rats. *J Comp Neurol* 1992;**320**:370–80.
16 **Berry M**, Hall S, Sievers J. Regeneration of axons in the mammalian visual system. *Brain Res* 1986;(Suppl)**13**:18–33.
17 **Crespo D**, O'Leary DDM, Cowan WM. Changes in the number of optic nerve fibres during late prenatal and postnatal development in the albino rat. *Dev Brain Res* 1985;**19**:129–34.
18 **Forrester J**, Peters A. Nerve fibres in optic nerve of rat. *Nature* 1967;**214**:245–7.
19 **Linden R**. Displaced ganglion cells in the retina of the rat. *J Comp Neurol* 1987;**258**:138–43.
20 **Perry VH**, Henderson Z, Linden R. Postnatal changes in retinal ganglion cell and optic axon populations in the pigmented rat. *J Comp Neurol* 1982;**219**:356–68.
21 **Potts RA**, Dreher B, Bennet MR. The loss of ganglion cells in the developing retina of the rat. *Dev Brain Res* 1982;**3**:481–6.
22 **Fukuda Y**, Sugimoto T, Shirokawa T. Strain differences in quantitative analysis of the rat optic nerve. *Exp Neurol* 1982;**75**:525–32.
23 **Eysel UT**. Susceptibility of the cat's visual system to hypoxia, hypotonia and ciculatory arrest. *Pflügers Arch* 1978;**375**:251–6.
24 **Grehn F**, Eysel UT. Patterns of ganglion cell loss after acute elevation of intraocular pressure in the cat. *Chibret Int J Ophthalmol* 1987;**5**:17–26.
25 **Gellrich NC**, Eysel UT, Machtens E. Damage to the optic nerve: an animal model. *Fortschr Kiefer Gesichtschir* 1996;**41**:1–6.
26 **Gellrich NC**. Controversies and state of the art in therapy of optic nerve lesions in craniofacial traumatology and surgery. *Mund Kiefer Gesichtschir* 1999;**3**:176–94.